

# Low Mass Dilepton Rate from the Deconfined Phase

Carsten Greiner<sup>a</sup>, Najmul Haque<sup>b</sup>, Munshi G. Mustafa<sup>a,b</sup>, and Markus H. Thoma<sup>c</sup>

<sup>a</sup>*Institut für Theoretische Physik, Johann Wolfgang Goethe University,*

*Max-von-Laue-Strasse 1, D-60438 Frankfurt, Germany*

<sup>b</sup>*Theory Division, Saha Institute of Nuclear Physics,*

*1/AF Bidhannagar, Kolkata 700 064, India and*

<sup>c</sup>*Max-Planck-Institut für extraterrestrische Physik,*

*Giessenbachstrasse, 85748 Garching, Germany*

## Abstract

We discuss low mass dilepton rates ( $\leq 1$  GeV) from the deconfined phase of QCD using both perturbative and non-perturbative models and compare with those from lattice gauge theory and in-medium hadron gas. Our analysis suggests that the rate at very low invariant mass ( $M \leq 200$  MeV) using the nonperturbative gluon condensate in a semiempirical way within the Green function dominates over the Born-rate and independent of any uncertainty associated with the choice of the strong coupling in perturbation theory. On the other hand the rate from  $\rho - q$  interaction in the deconfined phase is important between  $200 \text{ MeV} \leq M \leq 1 \text{ GeV}$  as it is almost of same order of the Born-rate as well as in-medium hadron gas rate. Also the higher order perturbative rate, leaving aside its various uncertainties, from HTL approximation becomes reliable at  $M \geq 200$  MeV and also becomes comparable with the Born-rate and the lattice-rate for  $M \geq 500$  MeV, constraining on the broad resonance structures in the dilepton rate at large invariant mass. We also discuss the lattice constraints on the low mass dilepton rate. Furthermore, we discuss a more realistic way to advocate the quark-hadron duality hypothesis based on the dilepton rates from QGP and hadron gas than it is done in the literature.

PACS numbers: 12.38.Cy,12.38.Mh,25.75.-q,11.10.Wx

Keywords: Quark-Gluon Plasma, Dilepton, Hard Thermal Loop Approximation, Gluon Condensate, Lattice Gauge Theory

## I. INTRODUCTION

The prime intention for ultra relativistic heavy-ion collisions is to study the behaviour of nuclear or hadronic matter at extreme conditions like very high temperatures and energy densities. A particular goal lies in the identification of a new state of matter formed in such collisions, the quark-gluon plasma (QGP), where the quarks and gluons are liberated from the nucleons and move freely over an extended space-time region. Various measurements taken in CERN-SPS [1] and BNL-RHIC [2–7] do lead to 'circumstantial evidence' for the formation of QGP. Evidence is (or can only be) 'circumstantial' because only indirect diagnostic probes exist.

Electromagnetic probes, such as real photon and dileptons, are a particular example, and accordingly thermal dileptons have been theoretically proposed long time ago [8]. At SPS energies [9] there was an indication for an enhancement of the dilepton production at low invariant mass ( $0.2 \leq M(\text{GeV}) \leq 0.8$ ) compared to all known sources of electromagnetic decay of the hadronic particles and the contribution of a radiating simple hadronic fireball (for comprehensive reviews see Refs. [10–12]). One of the possible explanations of this is the modification of the in-medium properties of the vector meson (*viz.*,  $\rho$ -meson) by rescattering in a hadronic phase along with only the lowest order perturbative rate, *i.e.*,  $q\bar{q}$  annihilation from a QGP [10–13]. Also at RHIC energies [3] a substantial amount of excess of electron pairs was reported in the low invariant mass region. Models taking into account in-medium properties of hadrons with various ingredients (see for details [14, 15]) can not explain the data from RHIC in the range  $0.15 \leq M(\text{GeV}) \leq 0.5$ , whereas they fit the SPS data more satisfactorily, indicating that a possible non-hadronic source becomes important at RHIC.

On the other hand, the higher order perturbative calculations [16] are also not very reliable at temperatures within the reach of the heavy-ion collisions. Moreover, perturbative calculations of the dilepton rate seem not to converge even in small coupling ( $g$ ) limit. Nevertheless, the lowest order perturbative  $q\bar{q}$  annihilation is the only dilepton rate from the QGP phase that is extensively used in the literatures. However, at large invariant mass this contribution should be dominant but not at low invariant mass, where nonperturbative effects should play an important role. Unfortunately, the lattice data [17] due to its limitations also could not shed any light on the low mass dileptons. However, the lattice calculations [18–20] provide evidence for the existence of nonperturbative effects associated

with the bulk properties of the deconfined phase, in and around the deconfined temperature,  $T_c$ . Also, indications have been found that the QGP at RHIC energies behaves more as a strongly coupled liquid than a weakly coupled gas [21]. Thus, a nonperturbative analysis of the dilepton rate from the deconfined phase is essential.

The dilepton emission at low invariant mass from the deconfined phase is still an unsettled issue in heavy-ion collisions at SPS and RHIC energies and, in particular, would be an important question for LHC energies and for compact baryonic matter formation in future FAIR energies [22], and also for the quark-hadron duality [10, 11, 23] that entails a reminiscence to a simple perturbative lowest order  $q\bar{q}$  annihilation rate [24]. In this article we reconsider the dilepton production rates within the perturbative QCD, and non-perturbative models based on lattice inputs and phenomenological  $\rho-q$  interaction in the deconfined phase. The analysis suggests that the nonperturbative dilepton rates are indeed important at the low invariant mass regime.

This article is organised in following way. In sec. II we discuss the dilepton production rate from the deconfined phase based on both perturbative and non-perturbative models. In sec. III we compare the momentum integrated rates from both QGP and Hadron gas (HG). We discuss the quark-hadron duality in sec. IV, and conclude in sec. V.

## II. DILEPTON RATE FROM DECONFINED PHASE

The dilepton production rate can be derived from the imaginary part of the photon self-energy [8, 25] as

$$\frac{dR}{d^4x d^4P} = -\frac{\alpha}{12\pi^4} \frac{1}{e^{E/T} - 1} \frac{\text{Im}\Pi_\mu^\mu(P)}{M^2}, \quad (1)$$

where  $\alpha = e^2/4\pi$  and  $P$  is four momentum of the virtual photon,  $E$  is its energy, and we use the notation  $P \equiv (p_0 = E, \vec{p})$  and  $p = |\vec{p}|$ . The square of the invariant mass of dilepton pair is  $M^2 = p_0^2 - p^2$ .

### A. Born Rate

To the lowest order the dilepton rate follows from one-loop photon self energy containing bare quark propagators. This rate corresponds to a dilepton production by the annihilation

of bare quarks and antiquarks of the QGP. Alternatively, this so-called Born-rate can also be obtained from the matrix element of the basic annihilation process folded with the thermal distribution functions of quarks. In the case of massless lepton pairs in a QGP with two massless quark flavours with chemical potential one finds [24]

$$\frac{dR}{d^4x d^4P} = \frac{5\alpha^2 T}{36\pi^4 p} \frac{1}{e^{E/T} - 1} \ln \frac{(x_2 + \exp[-(E + \mu)/T]) (x_1 + \exp[-\mu/T])}{(x_1 + \exp[-(E + \mu)/T]) (x_2 + \exp[-\mu/T])}, \quad (2)$$

where  $x_1 = \exp[-(E + p)/2T]$ ,  $x_2 = \exp[-(E - p)/2T]$ . A finite quark mass can easily be included.

For  $\mu = 0$  the dilepton rate becomes

$$\frac{dR}{d^4x d^4P} = \frac{5\alpha^2 T}{18\pi^4 p} \frac{1}{e^{E/T} - 1} \ln \left( \frac{\cosh \frac{E+p}{4T}}{\cosh \frac{E-p}{4T}} \right), \quad (3)$$

whereas that for total three momentum  $\vec{\mathbf{p}} = 0$  is given as

$$\frac{dR}{d^4x d^4P} = \frac{5\alpha^2}{36\pi^4} n(E/2 - \mu) n(E/2 + \mu), \quad (4)$$

with  $n(y) = (\exp(y) + 1)^{-1}$ , the Fermi-Dirac distribution function.

## B. Hard Thermal Loop perturbation theory (HTLpt) Rate

In order to judge the reliability of the lowest order result, one should consider higher order corrections. These corrections involve quarks and gluons in the photon self energy beyond the one-loop approximation. Using bare propagators at finite temperature, however, one encounters infrared singularities and gauge dependent results. These problems can be resolved, at least partially, by adopting the Hard-Thermal Loop (HTL) resummation scheme [26]. The key point of this method is the distinction between the soft momentum scale ( $\sim gT$ ) and the hard one ( $\sim T$ ), which is possible in the weak coupling limit ( $g \ll 1$ ). Resumming one-loop self energies, in which the loop momenta are hard (HTL approximation), effective propagators and vertices are constructed, which are as important as bare propagators if the momentum of the quark or gluon is soft. In HTLpt the bare  $N$ -point functions (propagator and vertices) are replaced by those effective  $N$ -point HTL functions which describe medium effects in the QGP such as the thermal masses for quarks and gluons and Landau damping.

The importance of the medium and other higher order effects on the dilepton rate depends crucially on the invariant mass and the momenta of the virtual photon. Therefore, we will discuss now the different kinematical regimes:

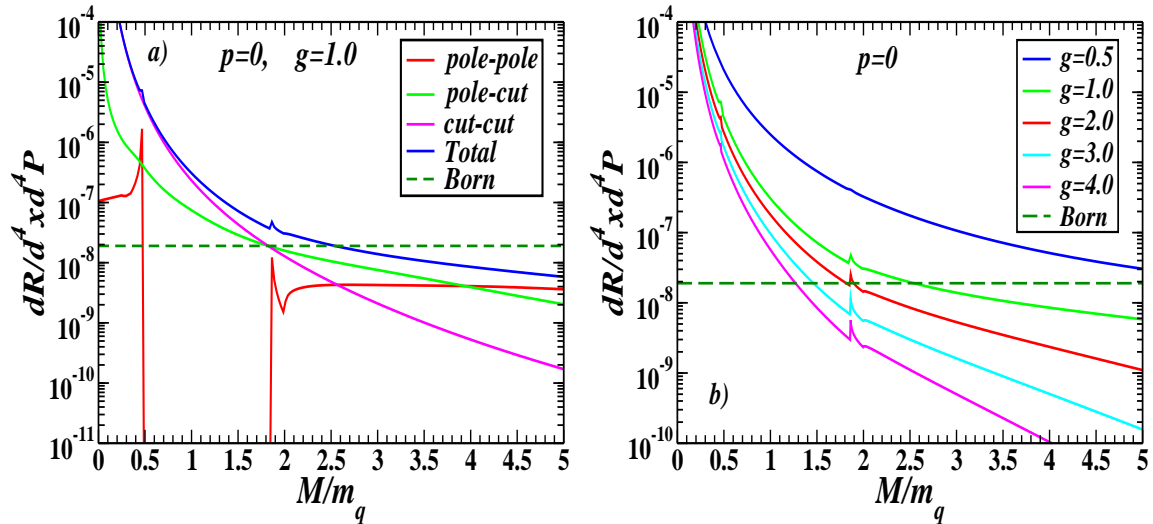


FIG. 1: (Color online) *Left panel (a)*: 1-loop dilepton rate for small invariant masses  $M \sim gT$  at zero momentum and Born-rate (dashed line) versus the scaled invariant photon mass  $M/m_q$  for  $g = 1$ . The van Hove peaks and energy gap are evident in the 1-loop rate. *Right panel (b)*: Total 1-loop rate for various  $g$  values.

### 1. Soft Rate ( $M \sim gT$ and $p \sim gT$ )

For soft invariant masses<sup>1</sup> and momenta of order  $gT$  one has to use HTL quark propagators and vertices in the one-loop photon self energy. These corrections are of same order as the Born-term [28]. Physically these corrections correspond to two different processes. First the poles of the HTL resummed quark propagators describe quasiparticles in the QGP with an effective thermal quark mass of the order of  $gT$ . Hence dileptons are generated by the annihilation of collective quark modes instead of bare quarks. In particular the HTL quark dispersion contains a so called plasmino branch which exhibits a minimum at finite

<sup>1</sup> Note that for ultrasoft  $M \sim g^2T$  and arbitrary momentum the rate is non-perturbative and cannot be calculated even within the HTL improved perturbation theory. This observation holds in particular for real hard photon [27].

momentum. This nontrivial dispersion leads to sharp structures (van Hove singularities and energy gap) in the dilepton production rate<sup>2</sup> in contrast to smooth Born-rate. Secondly, the imaginary part of the HTL quark self energy containing effective HTL  $N$ -point (propagators and quark-photon vertex) functions corresponds to processes involving the absorption or emission of thermal gluons.

In Fig. 1 the 1-loop dilepton rate for zero momentum, containing such processes, is displayed as a function of the scaled invariant mass with the thermal quark mass and is also compared with the Born-rate. In the left panel (Fig. 1(a)) the van Hove singularities due to the nontrivial dispersion of quarks in a medium are evident in pole-pole contributions whereas the pole-cut and cut-cut contributions<sup>3</sup> are smooth representing absorption and emission of gluons in the medium. The right panel (Fig. 1(b)) displays the total one-loop contribution for a set of values of  $g$ , where the energy gaps are smoothed due to the pole-cut and cut-cut contributions. Also the structures due to the van Hove singularities become also less prominent in the total contributions. The HTL rate, in particular, due to the cut contributions is also singular at  $M \rightarrow 0$  because the HTL quark-photon vertex is inversely proportional to photon energy.

However, these corrections are not sufficient and two-loop diagrams within HTL perturbation scheme contribute to the same order and are even larger than the one-loop results [16]. The total one- and two-loop rate at  $\vec{\mathbf{p}} = 0$  and  $M \ll T$  in the leading logarithm, *i.e.*,  $\ln(1/g)$  approximation reads [16, 32]

$$\frac{dR}{d^4x d^4P} = \frac{5\alpha^2 m_q^2}{9\pi^6 M^2} \left[ \frac{\pi^2 m_q^2}{4M^2} \ln \frac{T^2}{m_q^2} + \frac{3m_q^2}{M^2} \ln \frac{T^2}{m_g^2} + \frac{\pi^2}{4} \ln \left( \frac{MT}{M^2 + m_q^2} \right) + 2 \ln \left( \frac{MT}{M^2 + m_g^2} \right) \right], \quad (5)$$

where the thermal gluon mass is given by  $m_g^2 = 8m_q^2/3$  with  $m_q = gT/\sqrt{6}$ . Note that this expression is of the same order in  $g$  as the Born-term for soft  $M \sim gT$ . Now the Born-term for  $\vec{\mathbf{p}} = 0$  and  $M \ll T$  is simply given by

$$\frac{dR}{d^4x d^4P} = \frac{5\alpha^2}{144\pi^4} = 1.90 \times 10^{-8}. \quad (6)$$

In Fig. 2 the Born-rate and the complete two-loop rate for a set of values of  $g$  are

---

<sup>2</sup> For a discussion of van Hove singularities in the QGP at  $\vec{\mathbf{p}} = 0$  see Refs. [28–30] and also Ref. [31] for  $\vec{\mathbf{p}} \neq 0$ .

<sup>3</sup> These are due to the space-like ( $k^2 > k_0^2$ ) part of the  $N$ -point HTL functions that acquire a cut contribution from below the light cone.

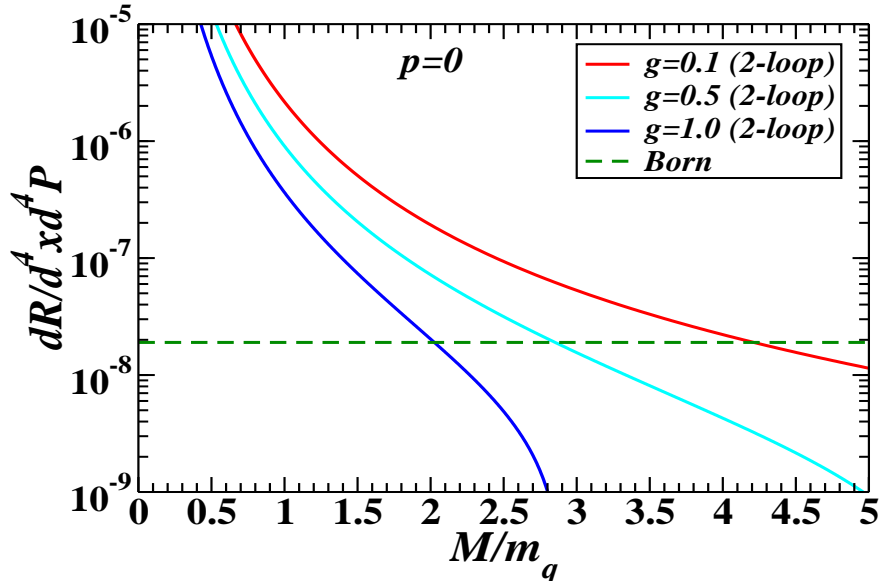


FIG. 2: (Color online) Complete 2-loop dilepton rate for small invariant masses  $M \sim gT$  at zero momentum and Born-rate (dashed line) versus the scaled invariant photon mass  $M/m_q$  with the thermal quark mass  $m_q$ .

compared. It is evident from Fig. 2 that the 2-loop rate dominates in the perturbative regime ( $g \leq 1$ ) over the Born-term for low mass domain,  $M/m_q \leq 2$ . However, the van Hove singularities contained in one-loop do not appear as they are washed out due to the leading logarithm approximation within the two-loop HTLpt.

## 2. Semi-hard Rate ( $M \sim T$ and $p \gg T$ )

For  $M$  of the order of  $T$  and hard momenta ( $p \gg T$ ), the  $\alpha_s$ -correction to the Born-rate has been calculated [33] within the HTLpt method as

$$\frac{dR}{d^4x d^4P} = \frac{5\alpha^2\alpha_s}{27\pi^3} \frac{T^2}{M^2} e^{-E/T} \left( \ln \frac{T(m_q + k^*)}{m_q^2} + C \right), \quad (7)$$

where  $k^* \approx |Em_q^2/M^2 - m_q^2/(4E)| < (E + p)/2$  and  $C \approx -0.5$  depends weakly on  $M$ . In Ref.[34] it has been shown that further corrections to the rate (7) are necessary. However, numerical results showed only a slight modification.

Assuming typical values of the strong coupling constant and temperature,  $T = 200$  MeV, these corrections dominate over the Born term for invariant masses below 300 MeV as shown

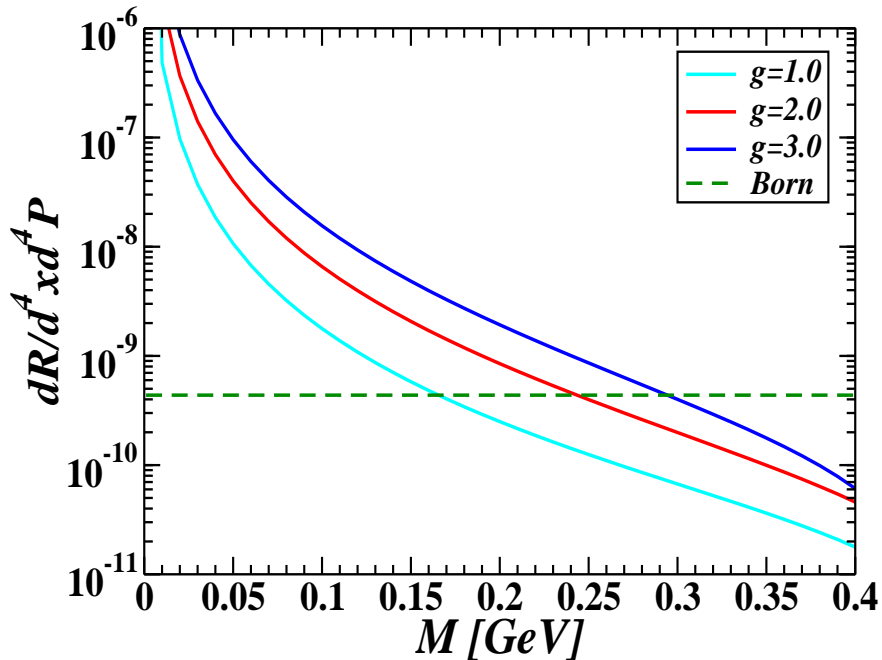


FIG. 3: (Color online)  $\alpha_s$ -correction to the dilepton rate and Born-rate (dashed line) versus the invariant photon mass  $M$  scaled with the thermal quark mass for  $T = 200\text{MeV}$  and  $E = 1 \text{ GeV}$ .

in Fig. 3. Similar results have been obtained using bare quark propagators [35]. However, the calculation within naive perturbation theory [36] resulted in  $\alpha_s$ -corrections which are of similar size as the Born-rate in the regime  $M$  and  $p$  of the order of  $T$ .

### 3. Hard Rate ( $M \gg T$ )

For  $M \gg T$  naive perturbation theory using bare propagators and vertices is sufficient. This is in contrast to the production of real photons, where one encounters an infrared singularity from bare quark propagator [37]. For finite  $M$ , however, this singularity cancels [38]. Bare two-loop calculations [36, 38] showed that the  $\alpha_s$ -corrections are negligible in this regime. However, a recent calculation of the  $\alpha_s$ -corrections [39] for large invariant mass  $M \gg T$  and small momenta  $p \ll T$  yielded important corrections to the Born-rate for invariant masses below  $(2 - 3)T$ . However, this work has also been criticized [40].

The main problem in applying perturbative results discussed above to realistic situations is the fact that  $g$  is not small but rather we have  $g \sim 1.5 - 2.5$ . Close to the critical



temperature,  $T_c$ , even  $g$  could be as high as 6 [41]. Hence the different momentum scales are not distinctly separated in the real sense and, even if one still believes in perturbative results (see Figs. 1 , 2 and 3) at least qualitatively, it is not clear which of the above rates applies to heavy-ion collisions. However, in all cases there are substantial corrections to the Born-rate. The perturbative rates within their uncertainties in various regime probably suggest that the Born-rate may not be sufficient for describing the low mass dilepton spectrum.

### C. Nonperturbative Rate

Considering the uncertainty of thermal perturbation theory for QCD a nonperturbative approach to the dilepton rate would be desirable. In this subsection we describe non-perturbative dilepton production rates in a deconfined phase in phenomenological models and in a first principle calculation, *viz.*, within the lattice gauge theory.

#### 1. Rate using Gluon Condensate within the Green Function

An important issue towards the understanding the phase structure of QCD is to understand the various condensates, which serve as order parameters of the broken symmetry phase. These condensates are non-perturbative in nature and lattice provides a connection with bulk properties of QCD matter. However, the quark condensate has a rather small impact on the bulk properties, *e.g.*, on the equation of state of QCD matter, compared to the gluon condensate [18]. The relation of the gluon condensate to the bulk properties such as equation of states, in principle, can be tested through hydrodynamic or transport properties sensitive to the equation of states, but is a non-trivial task.

A semi-empirical way to consider nonperturbative aspects, *e.g.* gluon condensate has been suggested by combining lattice results with Green function in momentum space [42, 43]. In this approach the effective  $N$ -point functions [42, 43] have been constructed which contain the gluon condensate in the deconfined phase, measured in lattice QCD [18]. The resulting quark dispersion relation with a mass  $m_q \sim 1.15T_c$  [42] in the medium shows qualitatively the same behaviour as the HTL dispersion, leading again to sharp structures (van Hove singularities, energy gap) in the dilepton production rates [44], indicating that this features are universal in relativistic plasmas independent of the approximation used [29]. In Fig. 4 the

dilepton production rate using gluon condensate is displayed for various values of momentum at  $T = 2T_c$  and also compared with the Born-rate. At very low invariant mass ( $M/T_c \leq 2$ ; for  $T_c \sim 165$  MeV,  $M \leq 330$  MeV) with realistic momentum the dilepton rate with gluon condensate dominates over the Born-rate. This rate will be important at very low invariant mass as it has non-perturbative input from lattice QCD that describes the bulk properties of the deconfined phase, and is of course free from any uncertainty related to the strong coupling  $g$  associated with the perturbative rates discussed in subsec. B.

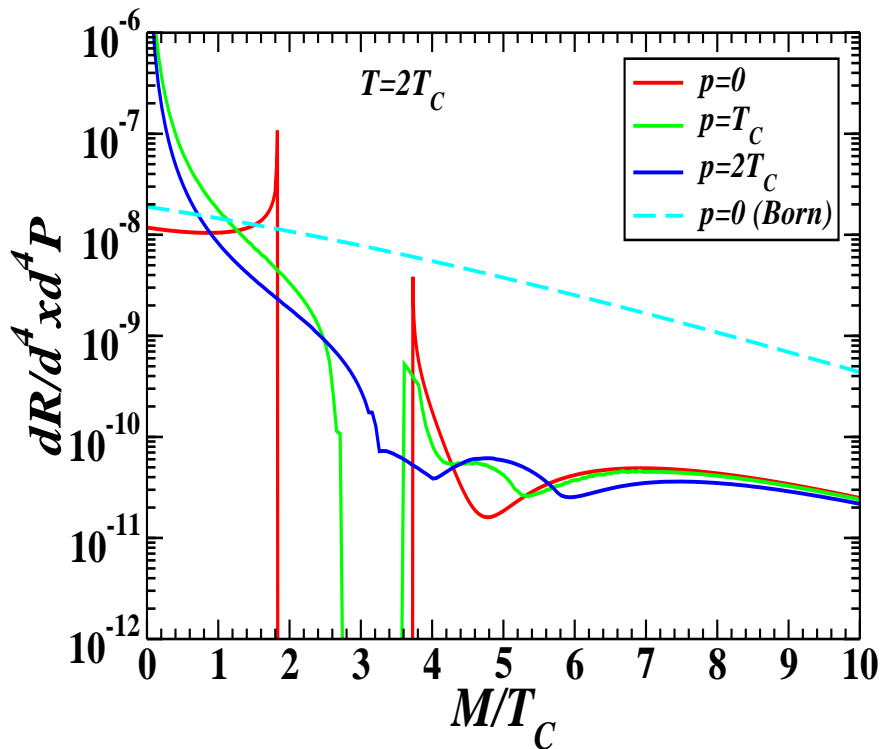


FIG. 4: (Color online) Van Hove singularities in the dilepton rate in the presence of gluon condensate as a function of invariant mass scaled with  $T_c$  for a set of momenta at  $T = 2T_c$ . The dashed curve is for Born-rate at zero momentum.

We, however, also note that the rate deviates from the Born-rate at high  $M/T_c$  ( $\geq 4$ ). The difference at high  $M/T_c$  has the origin in the asymptotic limit (large momentum  $k$ ) of the quark dispersion relation with gluon condensates. In this limit it is found that the normal quark mode behaves like  $w_+ = k + c$ , where  $c$  contains still the non-zero contribution from the condensates. The reason for which is the use of the momentum independent condensate

values. This fact has crept in the dilepton rate at high  $M/T_c$ . One way out could be to use an *ad hoc* separation scale ( $M/T_c \sim 2-3$ ) up to which one may employ the non-perturbative quark dispersion associated with the gluon condensate and beyond which a free dispersion is adopted. Alternatively, one could use a momentum dependent condensate, which is again beyond the scope of our calculation and has to be provided by the lattice analysis. To date we are not aware of such analysis. Nonetheless, we note that the nonperturbative contribution is important only at low invariant mass as we would see later in sec. III.

## 2. Quark and $\rho^0$ -meson Interaction ( $\rho$ -meson in QGP)

We assume that  $\rho$ -meson like states ( $q\bar{q}$  correlator in the  $\rho$ -meson channel) can exist in a deconfined phase like QGP. Then there will also be a contribution from  $\rho$ -meson channel to the dilepton pairs ( $l^+l^-$ ) in addition to the perturbative production. In order to consider such a channel phenomenologically an interaction of  $\rho - q$  coupling is introduced through the Lagrangian [45]

$$\mathcal{L} = -\frac{1}{4}\rho_{\mu\nu}^a\rho_a^{\mu\nu} + \frac{1}{2}m_\rho^2\rho_\mu^a\rho_a^\mu + \bar{q} \left( i\gamma_\mu\partial^\mu - m_q + G_\rho\gamma^\mu\frac{\tau_a}{2}\rho_\mu^a \right) q, \quad (8)$$

where  $q$  is the quark field,  $m_q$  is the quark mass,  $a$  is the isospin or flavour index, and  $\tau_a$  is the corresponding isospin matrix. The  $\rho - q$  coupling,  $G_\rho$ , can be obtained in the same spirit as the 4-point interaction,  $G_2(\bar{q}\gamma_\mu\tau_a q)^2$ , in NJL-model. This suggests  $G_\rho = \sqrt{8m_\rho^2 G_2} \sim 6$ , by taking  $G_2$  from the literature. The similar value for  $G_\rho$  can be obtained by simply assuming that the  $\rho$ -meson couples in a universal way to nucleons, pions and quarks [45].

Now using the Vector Meson Dominance (VMD) [25] the photon self-energy is related to the  $\rho^0$  meson propagator,  $D_{\mu\nu}(P)$ , by

$$\text{Im}\Pi_\mu^\mu(P) = \frac{e^2}{G_\rho^2} m_\rho^4 \text{Im}D_\mu^\mu(P) . \quad (9)$$

Then the thermal dilepton production rate from the  $\rho$ -meson can be written as

$$\frac{dR}{d^4x d^4P} = -\frac{1}{3\pi^3} \frac{\alpha^2}{G_\rho^2} \frac{m_\rho^4}{M^2} \frac{1}{e^{E_p/T} - 1} (\mathcal{A}_\rho^L + 2\mathcal{A}_\rho^T) , \quad (10)$$

and the spectral functions for  $\rho$ -meson can be obtained from the self-energy of  $\rho$ -meson as

$$\mathcal{A}_\rho^L(P) = \frac{\text{Im}\mathcal{F}}{(M^2 - m_\rho^2 - \text{Re}\mathcal{F})^2 + (\text{Im}\mathcal{F})^2} , \quad (11)$$

$$\mathcal{A}_\rho^T(P) = \frac{\text{Im}\mathcal{G}}{(M^2 - m_\rho^2 - \text{Re}\mathcal{G})^2 + (\text{Im}\mathcal{G})^2}, \quad (12)$$

where  $\mathcal{F} = -\frac{p^2}{p^2}\Pi^{00}(P)$  and  $\mathcal{G} = \Pi_T(P)$  with  $L$  and  $T$  stand for longitudinal and transverse modes, respectively.

Going beyond the HTL approximation, the integral expression for the matter part of the one-loop photon self energy for assymmetric charges in the deconfined phase (*viz.*, with non-zero chemical potential,  $\mu$ , which would be appropriate for FAIR energies [22]) can be obtained easily by extending the results of Ref. [45] to finite  $\mu$  as,

$$\begin{aligned} \text{Re } \mathcal{F} &= \frac{3G^2}{4\pi^2} \frac{M^2}{p^2} \int_0^\infty dk k [n(\omega_k - \mu) + n(\omega_k + \mu)] \left( -2\frac{k}{\omega_k} + \frac{M^2 + 4\omega_k^2}{4p\omega_k} \ln |a| + \frac{p_0}{p} \ln |b| \right), \\ \text{Im } \mathcal{F} &= \frac{3G^2}{4\pi} \frac{M^2}{p^3} \int_{k_-}^{k_+} dk k [n(\omega_k - \mu) + n(\omega_k + \mu)] \left( p_0 - \omega_k - \frac{M^2}{4\omega_k} \right), \\ \text{Re } \mathcal{G} &= \frac{3G^2}{4\pi^2} \int_0^\infty dk \frac{k^2}{\omega_k} [n(\omega_k - \mu) + n(\omega_k + \mu)] \left( - \left[ \frac{\omega_k^2 M^2}{2p^3 k} + \frac{M^2}{4pk} + \frac{M^4}{8p^3 k} + \frac{m_q^2}{2pk} \right] \ln |a| \right. \\ &\quad \left. - \frac{p_0 M^2 \omega_k}{2p^3 k} \ln |b| + \frac{M^2}{p^2} + 2 \right) \\ \text{Im } \mathcal{G} &= \frac{3G^2}{8\pi p} \int_{k_-}^{k_+} dk k [n(\omega_k - \mu) + n(\omega_k + \mu)] \left( -\omega_k + \frac{m_q^2}{\omega_k} + \frac{p_0^2}{p^2} \omega_k + \frac{M^2}{2\omega_k} \right. \\ &\quad \left. + \frac{M^4}{4\omega_k p^2} - \frac{p_0 M^2}{p^2} \right), \end{aligned} \quad (13)$$

along with

$$\begin{aligned} a &= \frac{(M^2 + 2pk)^2 - 4p_0^2 \omega_k^2}{(M^2 - 2pk)^2 - 4p_0^2 \omega_k^2}, \quad b = \frac{M^4 - 4(pk + p_0 \omega_k)^2}{M^4 - 4(pk - p_0 \omega_k)^2}, \\ k_- &= \frac{1}{2} \left| p_0 \sqrt{1 - \frac{4m_q^2}{M^2}} - p \right|, \quad k_+ = \frac{1}{2} \left( p_0 \sqrt{1 - \frac{4m_q^2}{M^2}} + p \right), \end{aligned}$$

where  $\omega_k = \sqrt{k^2 + m_q^2}$ .

In Fig. 5 the  $\rho$ -meson spectral function related to the imaginary part of the  $\rho$ -meson propagator (left panel) in (9) and the dilepton rate (right panel) are displayed for various temperature with  $\mu = 0$  and  $p = 200$  MeV. As the temperature increases the peak in the imaginary part of the  $\rho$ -meson propagator  $D$  becomes broader and is also reflected in the dilepton rate. In the low mass region ( $\leq 1$  GeV) the rate is comparable with the Born-rate.

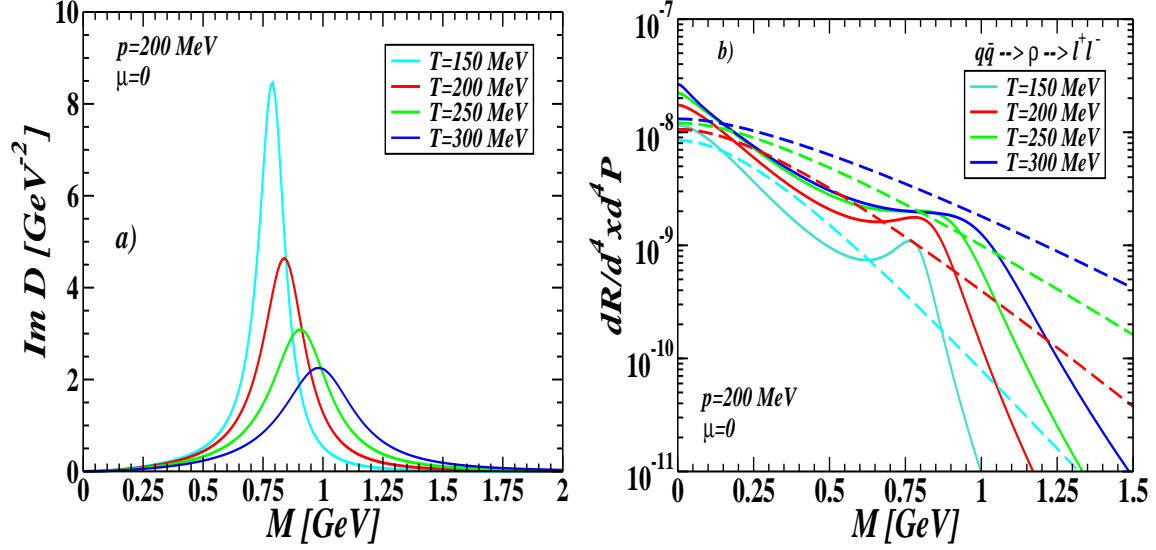


FIG. 5: (Color online) *Left panel:* Imaginary part of  $\rho$ -meson propagator (spectral function) as a function of the invariant mass  $M$  for a set of values  $T$ . *Right panel:* The dilepton rate from  $\rho$ -meson in a QGP as a function of  $M$ . The dashed lines are corresponding Born-rates. We have used  $G_\rho = 6$ .

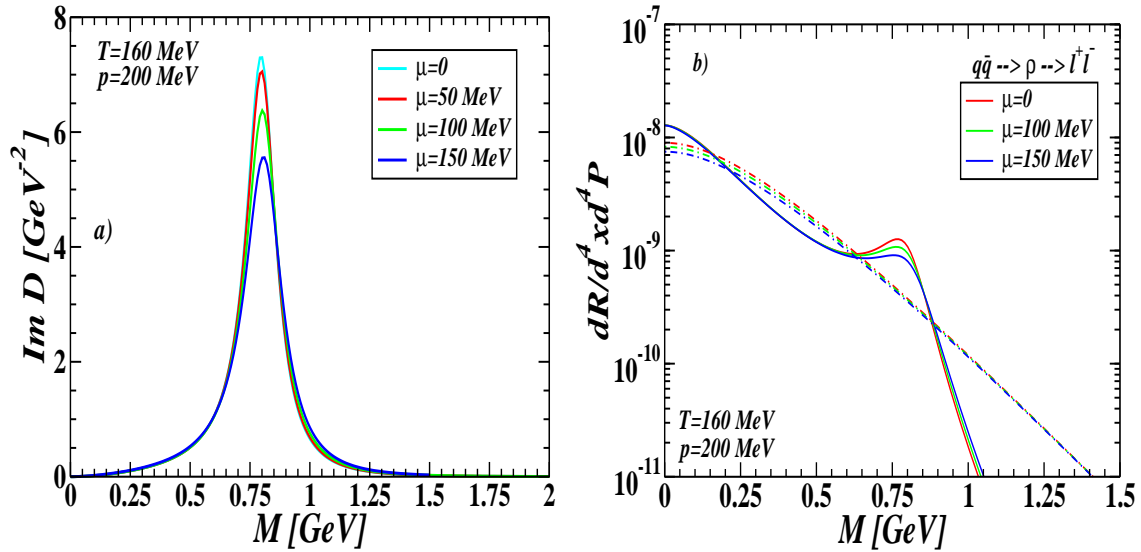


FIG. 6: (Color online) Same as Fig. 5 but for different  $\mu$  at a given  $T$ .

In Fig. 6 the  $\rho$ -meson spectral function (left panel) and the dilepton rate (right panel) are displayed for various  $\mu$  at  $T = 160$  MeV and  $p = 200$  MeV, which could be appropriate in the perspective of FAIR energies. The effect of broadening of the  $\rho$ -meson is far less pronounced with increasing  $\mu$  than increasing  $T$ , indicating that the  $\rho$ -meson is not completely melted

in the case of a system with finite baryon density such as expected at FAIR energies even above the phase transition. However, dilepton rates from  $\rho$ -meson as shown in Figs. 5 and 6 are comparable with the Born-rate in QGP in the low mass region ( $M \leq 1$  GeV), may be an indication for chiral restoration [10, 11, 45]. In addition this rate would be important for invariant masses below 1 GeV.

We also note that if one includes higher mass vector mesons such as  $\phi$ -meson within VMD, then there will be a peak corresponding to an invariant mass of the order of  $\phi$ -meson mass but in low mass region ( $M \leq 1$  GeV) there should be a very little change (less than 5%) in the dilepton rate. Since we are interested in the low mass region, we have not discussed  $\phi$ -meson here.

### 3. Rate from Lattice Gauge Theory

The thermal dilepton rate describing the production of lepton pairs with energy  $\omega$  and momentum  $\vec{\mathbf{p}}$  is related to the Euclidian correlation function [30] of the vector current,  $J_V^\mu = \bar{\psi}(\tau, \vec{\mathbf{x}})\gamma^\mu\psi(\tau, \vec{\mathbf{x}})$ , which can be calculated numerically in the framework of lattice gauge theory. The thermal two-point vector correlation function in coordinate space,  $\mathcal{G}_V(\tau, \vec{\mathbf{x}})$ , is defined as

$$\mathcal{G}_V(\tau, \vec{\mathbf{x}}) = \langle J_V(\tau, \vec{\mathbf{x}}) J_V^\dagger(\tau, \vec{\mathbf{x}}) \rangle = T \sum_{n=-\infty}^{\infty} \int \frac{d^3p}{(2\pi)^3} e^{-i(w_n\tau - \vec{\mathbf{p}} \cdot \vec{\mathbf{x}})} \chi_V(w_n, \vec{\mathbf{p}}) , \quad (14)$$

where the Euclidian time  $\tau$  is restricted to the interval  $[0, \beta = 1/T]$ , and the Fourier transformed correlation function  $\chi_V$  is given at the discrete Matsubara modes,  $w_n = 2\pi nT$ . The imaginary part of the momentum space correlator gives the spectral function  $\sigma_V(\omega, \vec{\mathbf{p}})$ , as

$$\chi_V(w_n, \vec{\mathbf{p}}) = - \int_{-\infty}^{\infty} \frac{\sigma_V(\omega, \vec{\mathbf{p}})}{i w_n - \omega + i\epsilon} \Rightarrow \sigma_V(\omega, \vec{\mathbf{p}}) = \frac{1}{\pi} \text{Im} \chi_V(\omega, \vec{\mathbf{p}}) . \quad (15)$$

Using (14) and (15) the spectral representation of the thermal correlation functions at fixed momentum in coordinate space can be obtained as

$$\mathcal{G}(\tau, \vec{\mathbf{p}}) = \int_0^\infty d\omega \sigma_V(\omega, \vec{\mathbf{p}}) \frac{\cosh[\omega(\tau - \beta/2)]}{\sinh[\omega\beta/2]} . \quad (16)$$

The vector spectral function,  $\sigma_V$ , is related to the differential dilepton production

rate [30]<sup>4</sup> as

$$\sigma_V(\omega, \vec{p}) = \frac{18\pi^2 N_c}{5\alpha^2} \omega^2 (e^{\omega/T} - 1) \frac{dR}{d^4x d^4P}, \quad (17)$$

where  $N_c$  is the number of color degree of freedom.

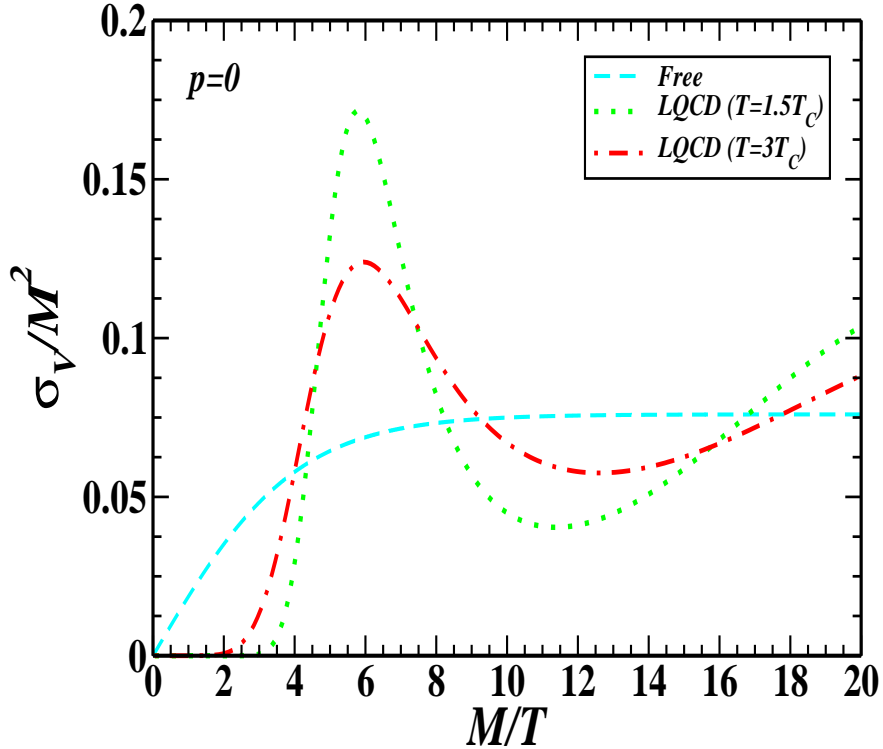


FIG. 7: (Color online) The zero momentum ( $\vec{p} = 0$ ) vector spectral function, reconstructed from the correlation function [17] within lattice gauge theory in quenched QCD using MEM, scaled with  $M^2$  as a function of  $M/T$  compared with that of the free one above the deconfinement temperature  $T_c$ .

A finite temperature lattice gauge theory calculation is performed on lattices with finite temporal extent  $N_\tau$ , which provides information on the temporal correlation function,  $\mathcal{G}(\tau, \vec{p})$ , only for a discrete and finite set of Euclidian times  $\tau = k/(N_\tau T)$ ,  $k = 1, \dots, N_\tau$ . The correlation function,  $\mathcal{G}(\tau, \vec{p})$ , has been computed [17] within the quenched approximation of QCD using non-perturbative improved clover fermions [46] through a probabilistic application based on the maximum entropy method (MEM) [47] for temporal extent  $N_\tau = 16$

<sup>4</sup> A factor of 2 differs from that of Ref. [17]

and spatial extent  $N_\sigma = 64$ . Then by inverting the integral in (16), the spectral function is reconstructed [17] in lattice QCD. In Fig.7 such a reconstructed spectral function scaled with  $M^2$  (equivalently  $\omega^2$  for  $\vec{p} = 0$ ) is displayed as a function of  $M/T$ . The vector spectral functions above the deconfinement temperature (*viz.*,  $T = 1.5T_c$  and  $3T_c$ ) show an oscillatory behaviour compared to the free one. The spectral functions are also found to be vanishingly small for  $M/T \leq 4$  due to the sharp cut-off used in the reconstruction.

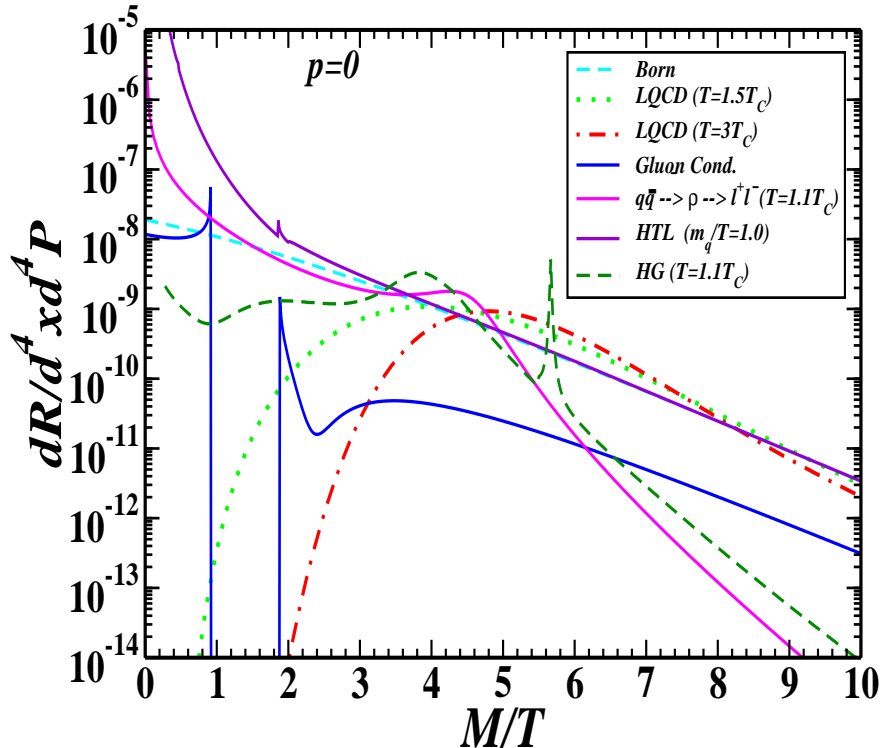


FIG. 8: (Color online) Comparison of various dilepton rates in a QGP and in a hadron gas (HG) as a function of  $M/T$  for momentum  $\vec{p} = 0$ . The critical temperature is 165 MeV [20] and the value of  $G_\rho$  is chosen as 6. The in-medium HG rate is from the recent calculations of Ref.[48].

A direct calculation of the differential dilepton rate using (17) above the deconfined temperature ( $T_c$ ) at  $\vec{p} = 0$  was first time done in Ref.[17] within the lattice gauge theory in quenched QCD using the MEM. In Fig. 8 the lattice dilepton rates at  $\vec{p} = 0$  for two temperatures ( $T = 1.5T_c$  and  $3T_c$ ) are displayed as a function of the scaled invariant mass with temperature and  $M/T = \omega/T$ , the energy of the dileptons. We have also compared the perturbative, non-perturbative and in-medium hadrons rates within the same normalisation



as shown in the plot. We note that the rate with gluon condensate perfectly scales with the temperature whereas that of HTL one depends on the choice of the effective coupling,  $m_q/T \sim g/\sqrt{6}$ . The lattice results are comparable within a factor of 2 with the Born-rate as well as that of HTLpt at high invariant mass  $M/T \geq 4$ . The absence of peak structures around the  $\rho$ -mass and also at higher  $M$  in the lattice dilepton rate probably constrain the broad resonance structures in the dilepton rates. However, for invariant mass below  $M/T \leq 4$  the lattice dilepton rate falls off very fast. This is due to the fact that the sharp cut-off is used to reconstruct the spectral function from the correlation function and the finite volume restriction in the lattice analysis. The lattice analysis is also based on rather small statistics. These lattice artefacts are related to the smaller invariant masses which in turn indicate that it is not yet very clear whether there will be any low mass thermal dileptons from the deconfined phase within the lattice gauge theory calculation. Future analysis could improve the situation in this low mass regime. One cannot rule out [17] the existence of van Hove singularities and energy gap, which are general features of massless fermions in a relativistic plasma [29], in the low mass dileptons. This calls for a further investigations on the lattice gauge theory side by improving and refining the lattice ingredients and constraints.

On the other hand, in HTLpt, apart from the uncertainty in the choice of  $g$ , the low mass ( $M \rightarrow 0$ , vanishing photon energy) one-loop dilepton rate obtained from vector meson spectral function analysis [30] diverges because the quark-photon vertex is inversely proportional to the photon energy. This also requires a further improvement of the HTLpt. However, we assume that the perturbative rate could also be reliable for  $M \geq 200$  MeV with  $T \geq 200$  MeV and  $g \geq 2$ . The other two phenomenological models, *viz.*, gluon condensate measured in lattice [18] and  $\rho - q$  interaction in the deconfined phase as discussed respectively above in subsec. C 1 and 2, for non-perturbative dilepton production at low mass regime are at least cleaner than the perturbative rates which depend weakly on the choice of the strong coupling constant. The rate with gluon condensate is free from strong coupling whereas that from  $\rho - q$  interaction does not depend strongly on the choice of the coupling (see below in Fig. 9). In addition to the perturbative rate these two together could also provide a realistic part of the dilepton rate at low mass regime ( $\leq 1$  GeV) from the deconfined phase, as also can be seen in the next section. As a comparison, we have also shown the recent rate from in-medium hadrons of Ref. [48], where the analytic structure of  $\rho$ -meson propagator has been used due to its interaction with thermal mesons.

### III. MOMENTUM INTEGRATED RATE

The momentum integrated dilepton rate can be obtained as

$$\frac{dR}{d^4x dM^2} = \int \frac{d^3p}{2p_0} \frac{dR}{d^4x d^4P}. \quad (18)$$

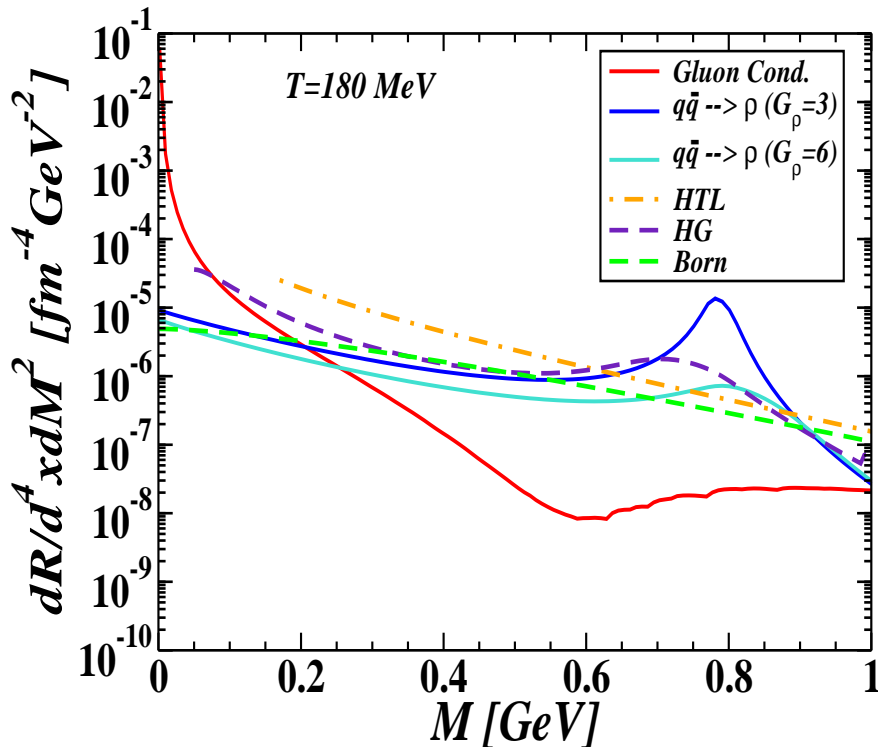


FIG. 9: (Color online) Momentum integrated dilepton rate as a function of the invariant mass  $M$ . We have used  $T_c = 165$  MeV for the nonperturbative rate with gluon condensate. The in-medium hadronic rate (HG) is from Ref. [48].

In Fig. 9 dilepton rates from QGP and in-medium hadrons are displayed as a function of invariant mass. As can be seen the non-perturbative contribution using gluon condensate dominates over Born-rate as well as the perturbative rate below  $M \leq 200$  MeV. The non-perturbative rate is indeed important with input from the first principle calculations [18] that describe the bulk properties of the deconfined phase. More importantly, this domain is also beyond reach of any reliable perturbative calculations in true sense. The rate from  $\rho - q$  interaction is almost of the same order as that of the Born-rate as well as the in-medium hadrons for  $M \leq 600$  MeV whereas it is higher than the perturbative one in the

domain  $600 \leq M(\text{MeV}) \leq 800$  due to the broadening of the  $\rho$  peak in the medium. We also note that this rate has a weak dependence on the realistic range of values of the  $\rho - q$  coupling (2 – 6). In addition the higher order perturbative rate from HTL, as discussed above, becomes reliable for  $M \geq 200$  MeV and also becomes of the order of Born-rate for  $M \geq 500$  MeV. We also note that the momentum integrated HTL rate used here has been obtained recently by Rapp et al. [11] through a parametrization of the prefactor of the zero momentum 1-loop HTL rate [28] with a temperature dependent  $g$ , which is claimed [49] to reproduce the Born-rate in (2) within the appropriate limit. Now for a comparison, we have also shown the recent rate from the in-medium hadrons of Ref. [48]. It is now clear that for low invariant mass ( $\leq 1$  GeV) only the Born-rate from the QGP is not realistic as well as insufficient for describing the dilepton rate. Instead we suggest that the non-perturbative rate with gluon condensate should be important for  $M \leq 200$  MeV whereas the rates from  $\rho - q$  interaction and HTLpt are important for  $M \geq 200$  MeV. Below we discuss some aspects of the quark-hadron duality hypothesis [23].

#### IV. THOUGHTS ON THE QUARK-HADRON DUALITY HYPOTHESIS

It is advocated [10, 23] that due to the potential broadening of the  $\rho$ -meson resonance suffering in a dense hadronic environment the overall (momentum integrated) dilepton rate out of the hadronic gas becomes equivalent to that from deconfined phase as

$$\frac{dR_H}{d^4x dM^2} \approx \frac{dR_Q}{d^4x dM^2} \quad , \quad (19)$$

which entails a reminiscence to a simple perturbative  $q\bar{q}$  annihilation in the vicinity of the expected QGP phase transition. This hypothesis of 'extended' quark-hadron duality for the thermal source of low mass dileptons has been claimed as an indication for chiral symmetry restoration [10, 11, 23] in the deconfined phase. However, we would like to note that in this hypothesis the volume of QGP and hadronic gas was assumed to be same in a given instant of time and therefore, the dileptons shine equally bright from both phases at a given instant of time per unit volume. This denotion of quark-hadron duality should be carefully re-addressed on its general validity, as the suggestive conclusion is indeed far-reaching. A more realistic way to look into it is envisaged below.

The momentum integrated rate in (18) shall be gauged to the adequate degrees of freedom

in a particular phase. A certain measure is given by the corresponding entropy density. Hence we suggest that for duality to hold one approximately should have

$$\frac{1}{s_H} \frac{dR_H}{d^4x dM^2} \approx \frac{1}{s_Q} \frac{dR_Q}{d^4x dM^2} \quad , \quad (20)$$

where  $s_i$  ( $i = H, Q$ ) is the entropy density of the respective phase. For an isoentropic crossing over the phase transition, one has  $s_H dV_H \approx s_Q dV_Q$ . Hence if one takes into account the respective volume of both phases at a given instant of time, then instead of (19) one should ask for

$$dV_H \frac{dR_H}{d^4x dM^2} \approx dV_Q \frac{dR_Q}{d^4x dM^2} \quad , \quad (21)$$

where  $dV_i$  ( $i = Q, H$ ) is the volume of the respective phase. Now, at a given instant of time this can lead to

$$\frac{dR_H}{dt dM} \approx \frac{dR_Q}{dt dM} \quad , \quad (22)$$

where  $dR_i/dt dM$  is the total yield per time from total phase  $i$  in the system at any instant of time. Therefore, equation (22) means that the fireball emits the same number of dileptons per unit time either if described by a hadronic or by a deconfined partonic description. This could likely be a more realistic way to look into the quark-hadron duality. Now, even if the momentum integrated rates in (18) from both phases are same in some kinematic domain (*e.g.*, see Fig. 9) may not necessarily imply a quark-hadron duality as given by (22) because hadronic volume is expected to be larger than that of QGP by at least a factor of 4 to 5. Furthermore, we also note that the quark-hadron duality should also be true for any momentum at a given instant of time.

## V. CONCLUSION

We have discussed the low mass dilepton production rate from the deconfined phase within various models, *viz.*, perturbative and non-perturbative, and compared with that of first principle calculations based on lattice gauge theory and in-medium hadrons. We also have discussed in details the limitations and uncertainties of all those models at various domains of the invariant mass. It turns out that at very low invariant mass ( $\leq 200$  MeV) the non-perturbative rate using gluon condensate measured in lattice becomes important as this domain is beyond reach of any reliable perturbative calculations. The other non-perturbative contribution from  $\rho - q$  interaction also becomes important below 1 GeV as it

is almost of same order as those of the Born and in-medium hadrons. We also note that these two rates are at least cleaner than the perturbative rates, in the sense that the gluon condensate rate has non-perturbative input from lattice equation of states and is thus free from any coupling uncertainties whereas the  $\rho - q$  interaction rate does not depend strongly on the choice of its coupling. We also discussed the  $\rho - q$  interaction in the perspective of FAIR scenario.

On the other hand the perturbative contribution, within its various uncertainties, becomes steady and reliable beyond  $M > 200$  MeV and also becomes comparable with the Born-rate and the LQCD rate for  $M \geq 500$  MeV. The LQCD rate also constrains the broad resonance structure at large invariant mass. More specifically, the rate with gluon condensate is important for  $M \leq 200$  MeV whereas those from the  $\rho - q$  interaction and HTLpt would be important for  $M \geq 200$  MeV for the deconfined phase in heavy-ion collisions. Instead of considering only the Born-rate the various nonperturbative and perturbative rates from appropriate domains of the invariant mass below 1 GeV would comprise a more realistic rate for low mass dileptons from the deconfined phase created in heavy-ion collisions. We hope that more elaborate future lattice gauge theory studies on dileptons above the deconfined temperature can provide a more insight than present LQCD calculations on the low mass region, which could then verify the various model calculations on low mass dileptons above the deconfined temperatures. Finally, we also have discussed a more realistic way to look into the quark-hadron duality hypothesis than it is advocated in the literature.

### Acknowledgments

The authors are thankful to S. Sarkar for providing the result of their calculations for in-medium hadron gas rate and P. Petreczky for also supplying the lattice data. MGM acknowledges various useful discussions and communications with H. van Hees. This work was partly supported by the Helmholtz International Centre for FAIR within the framework of LOEWE (Landes-Offensive zur Entwicklung Wissenschaftlich-ökonomischer Exzellenz)

program launched by the state of Hesse, Germany.

---

- [1] U. Heinz and M. Jacob, ‘*Evidence for a New State of Matter: An Assessment of the Result from CERN SPS Lead Beam Program*’,  $\langle$  nucl-th/0002042  $\rangle$ .
- [2] I. Arsene *et al.* (BRAHMS Collaboration), Nucl. Phys. **A757**, 1 (2005); K. Adcox *et al.* (PHENIX Collaboration), *ibid.* **757**, 184 (2005); B. B. Back *et al.* (PHOBOS Collaboration), *ibid.* **757**, 28 (2005); J. Adams *et al.* (STAR Collaboration), *ibid.* **757**, 102 (2005).
- [3] PHENIX Collaboration, A. Adare *et al.*, Phys. Rev. C **81**, 034911 (2010).
- [4] PHENIX Collaboration, S. S. Adler *et al.*, Phys. Rev. Lett. **98**, 012002 (2007).
- [5] PHENIX Collaboration A. Adare *et al.*, Phys. Rev. Lett. **98**, 162301 (2007).
- [6] PHENIX Collaboration, K. Adcox *et al.*, Phys. Rev. Lett. **88**, 022301 (2002); STAR Collaboration, C. Adler *et al.*, Phys. Rev. Lett. **89**, 092302 (2002).
- [7] PHENIX Collaboration, S. S. Adler *et al.*, Phys. Rev. Lett. **91**, 172301 (2003); T. Chujo, PHENIX Collaboration, Nucl. Phys. **A715**, 151c (2003).
- [8] L. McLerran and T. Toimela, Phys. Rev. D **31**, 545 (1985).
- [9] CERES Collaboration, G. Agakichiev *et al.*, Phys. Rev. Lett. **75**, 1272 (1995); Phys. Lett. **B422**, 405 (1998); N. Maseru for the HELIOS-3 Collaboration, Nucl. Phys. A **590**, 93c (1995); A. Drees for the CERES collaboration, Nucl. Phys. **B630**, 449c (1998).
- [10] R. Rapp and J. Wambach, ‘*Chiral Symmetry Restoration and Dileptons in relativistic Heavy-Ion Collisions*’, Adv. Nucl. Phys. **25**, 1 (2000).
- [11] R. Rapp, J. Wambach, and H. van Hees, ‘*The Chiral Restoration Transition of QCD and Low Mass Dileptons*’, arXiv:0901.3289.
- [12] W. Cassing and E. L. Bratkovskaya, Phys. Rep. **308**, 65 (1999).
- [13] G. E. Brown and M. Rho, Phys. Rev. Lett. **66**, 2720 (1991); B. Friman and H. J. Priner, Nucl. Phys. **A617**, 496 (1997); R. Rapp, G. Chanfray, and J. Wambach, Nucl. Phys. **A617**, 472 (1997); Phys. Rev. Lett. **76**, 368 (1996); C. Gale and P. Lichard, Phys. Rev. D **49**, 3338 (1994); R. Rapp and C. Gale, Phys. Rev. C **60**, 024903 (1999); F. Klingl, N. Kaiser, and W. Wiese, Nucl. Phys. **A624**, 527 (1997); W. Peters, M. Post, H. Lenske, S. Leupold, and U. Mosel, Nucl. Phys. **A632**, 109 (1998); W. Cassing, E. L. Bratkovskaya, R. Rapp, and J. Wambach, Phys. Rev. C **57**, 916 (1998); M. Post, S. Leupold, and U. Mosel, Nucl. Phys. A

- 689**, 753 (2001); V. Koch, M. Bleicher, A. K. Dutt-Mazumder, C. Gale and C. M. Ko, in *Hirscheegg 2000, Hadrons in dense matter*, p.136; D. K. Srivastava, B. Sinha, and C. Gale, Phys. Rev. C**53**, 567 (1996); D. Pal, D. K. Srivastava, and K. Haglin, Phys. Rev. C**54**, 1366 (1996); D. K. Srivastava, B. Sinha, D. Pal, C. Gale, and K. Haglin, Nucl. Phys. A**610**, 350c (1996); D. Pal and M. G. Mustafa, Phys. Rev. C**60**, 034905 (1999); D. K. Srivastava, M. G. Mustafa, and B. Müller, Phys. Rev. C**56**, 1064 (1997); J. Alam, S. Sarkar, P. Roy, T. Hatsuda, and B. Sinha, Ann. Phys. **286**, 159 (2001); J. Alam, P. Roy and S. Sarkar, Phys. Rev. C**67**, 054901 (2003).
- [14] K. Dusling and I. Zahed, Nucl. Phys. A**825**, 212 (2009).
- [15] E. L. Bratkovskaya, W. Cassing, and O. Linnyk, Phys. Lett. B**670**, 428 (2009).
- [16] P. Aurenche, F. Gelis, R. Kobes, and H. Zaraket, Phys. Rev. D**58**, 085003 (1998).
- [17] F. Karsch, E. Laermann, P. Petreczky, S. Stickan, and I. Wetzorke, Phys. Lett. B **530**, 147 (2000).
- [18] G. Boyd *et al.*, Nucl. Phys. B**469**, 419 (1996).
- [19] C. R. Alton *et al.*, Phys. Rev. D **68**, 014507 (2003); C. R. Alton *et al.*, Phys. Rev. D **71**, 054508 (2005); A. Bazavov *et al.*, Phys. Rev. D**80**, 014504 (2009); MILC Collaboration, C. Bernard *et al.*, Phys. Rev. D**71**, 034504 (2005).
- [20] P. Petreczky, Nucl. Phys. A**830**, 11c (2009); P. Petreczky, arXiv:1009.5935.
- [21] M. H. Thoma, J. Phys. G**31**, L7 (2005).
- [22] [http://www.gsi.de/portrait/fair\\_e.html](http://www.gsi.de/portrait/fair_e.html)
- [23] R. Rapp and J. Wambach, Eur. Phys. J. A**6**, 415 (1999).
- [24] J. Cleymans, J. Fingberg, and K. Redlich, Phys. Rev. D**35**, 2153 (1987).
- [25] C. Gale and J. Kapusta, Nucl. Phys. B**357**, 65 (1991).
- [26] E. Braaten and R. D. Pisarski, Nucl. Phys. B**337**, 569 (1990); Phys. Rev. Lett. **64**, 1338 (1990).
- [27] P. Aurenche, F. Gelis, and H. Zaraket, Phys. Rev. D**61**, 116001 (2000).
- [28] E. Braaten, R. D. Pisarski, and T. C. Yuan, Phys. Rev. Lett. **64**, 2242 (1990).
- [29] M. H. Thoma, Nucl. Phys. (Proc. Suppl.) B**92**, 162 (2001); M. G. Mustafa and M. H. Thoma, Pramana **60**, 711 (2003); A. Peshier and M. H. Thoma, Phys. Rev. Lett. **84**, 841 (2000).
- [30] F. Karsch, M. G. Mustafa, and M. H. Thoma, Phys. Lett. B**497**, 249 (2001).
- [31] S. M. H. Wong, Z. Phys. C**53**, 465 (1992).

- [32] P. Aurenche, F. Gelis, R. Kobes, and H. Zaraket, Phys. Rev. D**60**, 076002 (1999).
- [33] M. H. Thoma and C. Traxler, Phys. Rev. D**56**, 198 (1997).
- [34] M. E. Carrington, A. Gynther and P. Aurenche, Phys. Rev. D**77**, 045035 (2008); P. Aurenche, F. Gelis, G. D. Moore, and H. Zaraket, J. High. Energy Phys. **12**, 006 (2002); J. High. Energy Phys. **07**, 063 (2002).
- [35] T. Altherr and P. V. Ruuskanen, Nucl. Phys. B**380**, 377 (1992).
- [36] J. Cleymans, I. Dadic, and J. Joubert, Phys. Rev. D**49**, 230 (1994); J. Cleymans and I. Dadic, Phys. Rev. D**47**, 160 (1993).
- [37] J. I. Kapusta, P. Lichard, and D. Seibert, Phys. Rev. D **44**, 2774 (1992); R. Baier, H. Nakagawa, A. Niegawa, and K. Redlich, Z. Phys. C**53**, 433 (1992).
- [38] T. Altherr and P. Aurench, Z. Phys. C**45**, 99 (1989).
- [39] J. I. Kapusta and S. M. H. Wong, Phys. Rev. C**62**, 027901 (2000).
- [40] P. Aurenche *et al.*, Phys. Rev. D**65**, 038501 (2002).
- [41] A. Peshier, B. Kämpfer, O. P. Pavlenko, and G. Soff, Phys. Lett. B **337**, 235 (1994); Phys. Rev. D**54**, 2399 (1996); U. Heinz and P. Levai, Phys. Rev. C**57**, 1987 (1998).
- [42] A. Schäfer and M. H. Thoma, Phys. Lett. B**451**, 195 (1999).
- [43] M. G. Mustafa, A. Schäfer and M. H. Thoma, Phys. Lett. B**472**, 402 (2000).
- [44] M. G. Mustafa, A. Schäfer and M. H. Thoma, Phys. Rev. C**61**, 024902 (1999); Nucl. Phys. A**661**, 653 (1999).
- [45] M. H. Thoma, S. Leupold, and U. Mosel, Eur. Phys. J A**7**, 219 (2000)
- [46] B. Sheikholeslami and R. Wohlert, Nucl. Phys. B**259**, 572 (1985); M. Lüster *et al.*, Nucl. Phys. B**491**, 344 (1997).
- [47] Y. Nakahara, M. Asakawa, and T. Hatsuda, Phys. Rev. D**60**, 091503 (1999); M. Asakawa, T. Hatsuda, and Y. Nakahara, Prog. Part. Nucl. Phys. **46**, 459 (2001); I. Wetzorke, F. Karsch, in: C. P. Korthals-Altes (Ed.), Proceedings of the International Workshop on Strong and Electroweak Matter, World Scientific, 2001, p.193.
- [48] S. Ghosh, S. Sarkar, and J. Alam, arXiv:1009.1260.
- [49] H. van Hees: Private communication